Nuclear Engineering and Technology 54 (2022) 2564–2571

Contents lists available at ScienceDirect

Nuclear Engineering and Technology

journal homepage: www.elsevier.com/locate/net

Original Article

The detection efficiency study of NaI(Tl) scintillation detector with the different numbers of SiPMs

Bao Wang [a, b], Xiongjie Zhang [a, b, *], Qingshan Wang [a], Dongyang Wang [a], Dong Li [a, b], Mingdong Xiahou [a, b], Pengfei Zhou [a], Hao Ye [a], Bin Hu [a], Lijiao Zhang [a]

[a] Engineering Research Center of Nuclear Technology Application (East China University of Technology), Ministry of Education, Nanchang, 330013, China
[b] School of Mechanical and Electronic Engineering, East China University of Technology, Nanchang, 330013, China

ARTICLE INFO

Article history:
Received 7 October 2021
Accepted 5 January 2022
Available online 7 January 2022

Keywords:
Gamma spectrometer
NaI(Tl)
SiPM
Energy resolution

ABSTRACT

SiPMs are generally coupled into whole columns in gamma energy spectrum measurement, but the relationship between the distribution of whole SiPM columns and the energy resolution of the measured energy spectra is rarely reported. In this work, ⌀ 3 × 3 inch NaI scintillator is placed on an 8 × 8 SiPM array, and the energy resolution of the ^{137}Cs peak at 662 keV corresponding to the γ-ray is selected as a reference. Each SiPM is switched to explore the influence of the number of SiPM arrays, distribution position, and reflective layer on the energy resolution of SiPMs. Results show that without coupling, the energy resolution is greatly improved when the number of SiPMs ranges from 4 to 32. However, after 32 slices (the area covered by SiPMs relative to the scintillator reaches 25.9%), the improvement in energy resolution and total pulse count is not obvious. In addition, the position of SiPMs relative to the scintillator does not exert much impact on the energy resolution. Results also indicate that by adding a reflective film (ESR), the energy resolution of the tested group increases by 10.38% on average. This work can provide a reference for the design and application of miniaturized SiPM gamma spectrometers.

1. Introduction

Scintillation detectors are currently the most widely used radiation detectors. These detectors generally need to be coupled with photomultiplier tubes (PMTs) to convert weak light signals into electrical signals for related measurements [1]. In recent years, silicon photo multipliers (SiPMs) have become a research hotspot because of their small size, low working voltage (the typical working voltage of PMTs is 400–1500 V, whereas that of SiPMs is 50 V or lower), high photon detection efficiency, and insensitivity to magnetic fields. SiPMs can be used in fluorescence detection, flow cytometry, wafer surface inspection, and particle size measurement [2,3]. Fig. 1 shows the schematic of the SiPM principle. A monolithic SiPM is composed of thousands of microcells connected in parallel. Each microcell contains an avalanche photodiode (APD) that works in Geiger mode and is connected to a quencher. All APDs are connected in parallel to form a whole, and the output pulses are superimposed on one another so that the output signal and photon absorption form a certain proportional relationship [4].

The size of current single-chip SiPMs is generally less than 1 cm^2. Multiple SiPMs are usually used to form arrays for collecting the fluorescence generated by NaI (Tl) scintillators with maximum performance [5]. For example, C. Kim et al. used 32 SiPMs to form an array coupled with a ⌀ 2 × 2 inch scintillator, and T. Huang et al. used 64 SiPMs to form an array coupled with a ⌀ 3 × 3 inch scintillator [6,7]. Z. Lin et al. also discussed the relationship between 4, 8, 16, and 32 SiPM arrays and the energy resolution of the measured energy spectra [8]. According to existing research, the greater the number of SiPMs is, the better the energy resolution of the measured energy spectra will be. However, the relationship between the distribution of SiPM arrays and the energy resolution of the measured energy spectra is rarely investigated.

Therefore, the current work designs a γ energy spectrum acquisition system that can control each SiPM chip. In addition, the relationship between the number of SiPM arrays, distribution position, reflective layer, and energy resolution of the measured energy spectra is explored, and the optimal design method for SiPM arrays is discussed. The results provide a theoretical basis for the promotion and application of SiPMs.

* Corresponding author. Engineering Research Center of Nuclear Technology Application (East China University of Technology), Ministry of Education, Nanchang, 330013, China.
E-mail address: xjzhang@ecut.edu.cn (X. Zhang).

https://doi.org/10.1016/j.net.2022.01.010

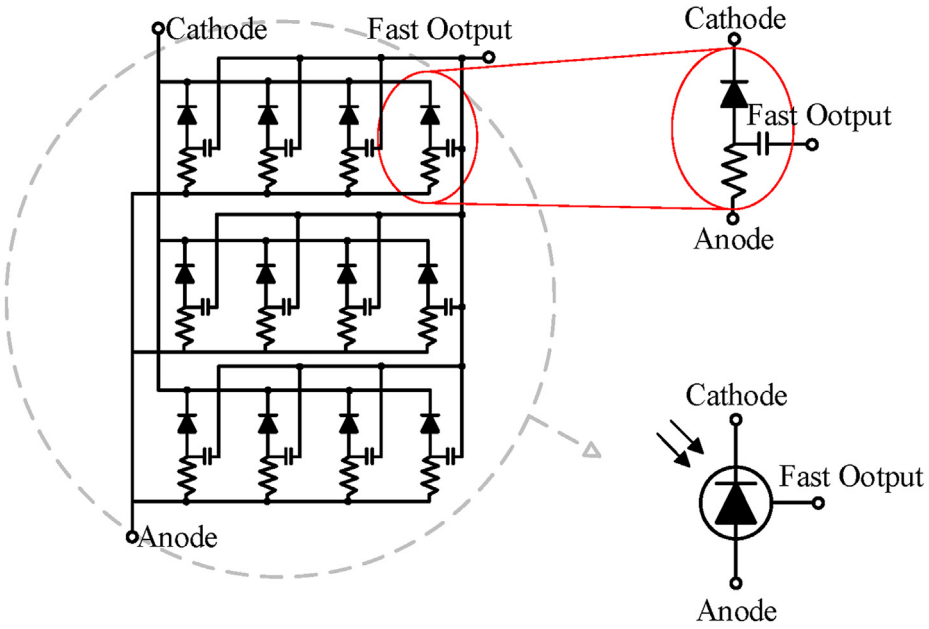

Fig. 1. Schematic of the internal principle of SiPMs.

2. Experimental system design and testing

2.1. System construction

To explore the optimization of SiPM arrays, we designed the SiPM energy spectrum acquisition system as follows: NaI (TI) scintillators are placed directly on an 8 × 8 square SiPM array, and the electrical signals generated by the SiPMs are sent to the summing circuit, which is finally connected to the back circuit. The backend circuit involves amplification, differential, ADC acquisition, and FPGA processing. This circuit is connected to a computer through the ARM, and the data collected in real time are sent to the upper computer. The visual information, such as the energy spectrum, is obtained after computer processing. Fig. 2 shows the complete system schematic. To facilitate the experiment, the computer provides power to the entire device. In the schematic, the black line (solid line) represents the power line, and the blue line (dashed line) represents the data line. We designed a set of experimental equipment, as shown in Fig. 3. SiPMs are extremely sensitive to photons. Hence, interference from external light during experiments should be avoided. Therefore, the equipment marked by the dashed box in Fig. 2 is operated in a lightproof box, as shown in Fig. 3 (right).

2.2. SiPM array and DIP switch design

The detection component is composed of a scintillator and a SiPM array. The scintillator can convert radiation into photons, and the resulting photons are further collected by SiPMs to generate electrical signals [9]. To determine the influence of the relative area between SiPMs and NaI crystals on the energy resolution, this study adopted a ⌀ 3 × 3 inch NaI scintillator. The SiPM array used in the study was J-60035 from ON Semiconductor. Table 1 lists some of the main parameters of the SiPMs. The selected monolithic size for the SiPMs was 6 mm × 6 mm. To cover the ⌀ 3 × 3 inch NaI crystal, we designed 64 SiPMs that form an 8 × 8 square array. The NaI and SiPM arrays are shown in Fig. 4. The discrete type of working voltage between SiPMs is very small, and the individual discrete type within the same array is much smaller. Generally, multiple SiPMs can use the same working voltage [10]. The SiPMs 'power supply part uses Hamamatsu's C14156 chip, which can output voltages up to 80 V by applying control voltage and power supply

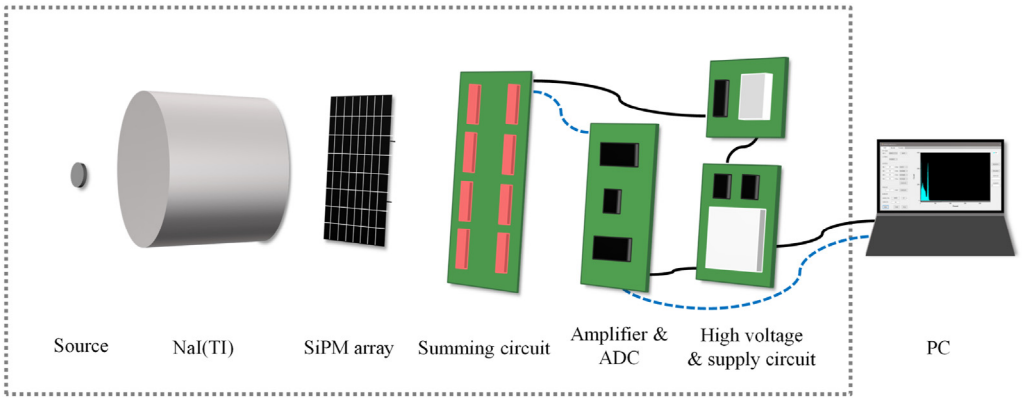

Fig. 2. Schematic of the experimental system.

Fig. 3. (Left) Internal diagram of experimental equipment; (Right) Lightproof box.

Table 1
Main parameters of the used SiPM array.

Manufacturer	SensL
Model	J-60035
Number of channels	64 (8 × 8 ch)
Active area/channel	6.07 × 6.07 mm^2
No. of Microcells	22,292
APD cell size	35 um
Microcell fill factor	75%
Rated gain	6.3 × 10^6
Spectral range	200–900 nm
Maximum sensitivity	420 nm

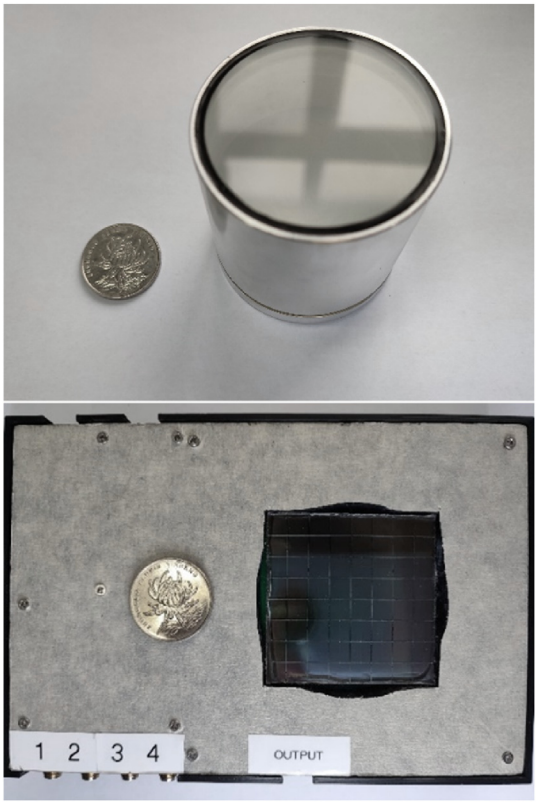

Fig. 4. (Top) ⌀ 3 × 3 inch NaI crystal; (Bottom) 8 × 8 inch SiPM array.

voltage. In the test herein, the SiPM bias voltage was set to 28 V (overvoltage = 3.5 V).

In investigating the relationship between the number of SiPMs and detection efficiency, the on–off status of each SiPM needs to be controlled. Therefore, the novelty of this design circuit lies in the addition of a DIP switch for each SiPM. Specifically, eight groups of 64 switches can individually control the on and off status of SiPMs. Fig. 5 (top) shows that control can be achieved by pressing and pulling up the mechanical switch. The output signal of each SiPM is summed during circuit design. Fig. 5 (bottom) shows a schematic of the summation circuit. Three signals are used as an example, while the remaining SiPM signals are omitted.

2.3. Design of preamplification circuit and AD acquisition circuit

As the signals collected by SiPMs are weak, summed signals need to be amplified. In this work, the AD8009 chip produced by Analog Devices was used in circuit amplification. The signal was amplified and sent to the differential circuit. The chip of the differential circuit was obtained from the AD8138 chip of the same company. Finally, the differential signal was sent to the 12-bit AD acquisition chip. The physical diagram of the preamplifier circuit and AD acquisition circuit is shown in Fig. 6.

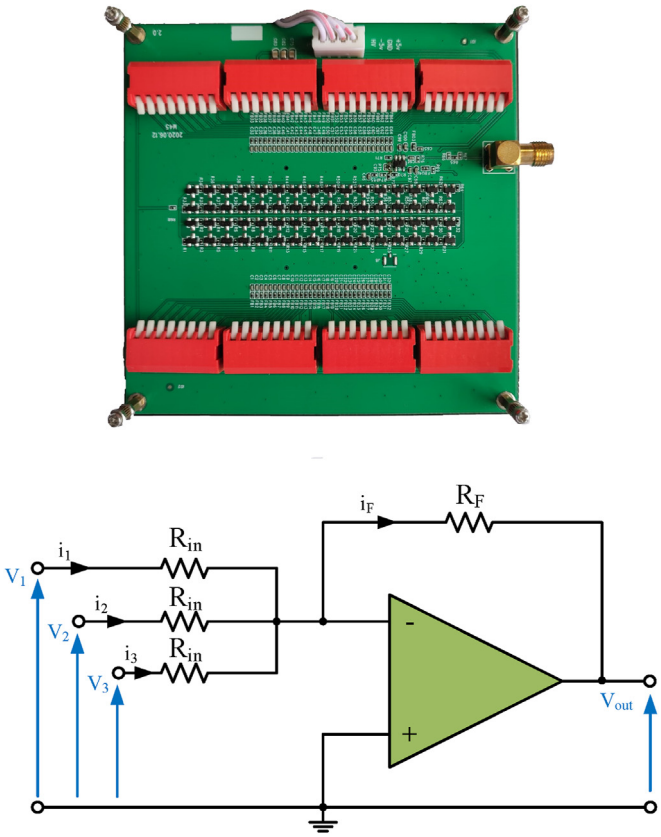

Fig. 5. (Top) SiPM DIP switch control board; (Bottom) Summing circuit model (three signals are taken as an example while the remaining signals are omitted).

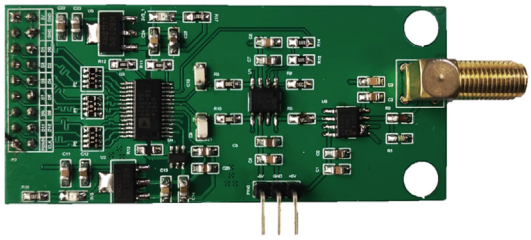

Fig. 6. Preamplifier and AD acquisition board.

2.4. Verification and testing

After the experimental device was built, the overall system was tested. Fig. 7 shows the energy spectrum of the uranium ore measured when all 64 SiPMs were turned on. From the collected map, we noted that the key characteristic peaks of uranium ore were clearly distinguishable. The characteristic peaks corresponding to 609.32, 1120.29, 1764.49, and 2204.06 keV are marked in the figure. The results verified that the experimental device could generate good energy spectra.

3. Materials and methods

3.1. Source selection

We select three radioactive sources for testing: ^{137}Cs, ^{241}Am, and uranium ore. Uranium ore is used for energy spectrum calibration. When the number of SiPMs is large, ^{241}Am is selected to verify the calibration results. Finally, the energy resolution of the 662 keV peak corresponding to ^{137}Cs is obtained [8]. In each case, 120S effective pulse counting is performed on ^{137}Cs. As the position of the source influences the test results, the placement position should remain the same each time, and the radioactive source should be placed directly above the center of the scintillator during the test [11].

3.2. Quantity selection

As SiPMs are relatively sensitive to temperature, all experimental equipment is placed in a thermostat for operation, and the temperature is set to 20 °C. In the whole test process, we ensure that the SiPM bias voltage is uniform at a precise and determined value. To study the relationship between the number of SiPM arrays and the energy resolution of the measured energy spectrum, we aim to test different numbers of SiPMs. The numbers of SiPMs tested are 1, 2, 3, 4, 8, 16, 32, 44, and 64. The numbers of opened SiPMs tested showed a trend of expanding from the center to the four sides. The corresponding positions of the different numbers of SiPMs are shown in Fig. 8. The change in color or increase in number in the figure denotes an increase in number. For example, when the number of SiPMs tested is 16, the SiPMs corresponding to 1 to 6 in the picture are included.

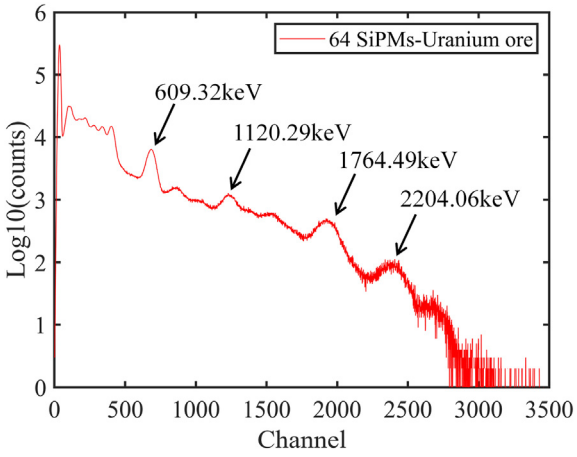

Fig. 7. Energy spectrum of uranium ore with 64 SiPMs turned on.

3.3. Location choice

To study the relationship between the distribution position of SiPM arrays and the energy resolution of measured energy spectra, we set up a position experiment. Symmetry needs to be considered when studying locations. As the number of SiPMs used is an 8 × 8 array, the selectivity provided is only 2, 4, 8, 16, and so on. In the case of ensuring the number of experimental groups and detection rate, we choose to turn on 8 slices to explore the positional influence of SiPMs. In the same environment as the quantitative study, we select 8 SiPMs for energy spectrum testing at different positions and divide them according to the distance from the center point. The corresponding position is shown in Fig. 9. The change of color or number in the figure denotes the change in position. In the figure, 1, 2, and 3 represent three different positions from the center point.

3.4. Addition of a reflective layer

On the basis of quantitative research, we continue to study whether adding a reflective layer will affect the energy detection rate. As the quantity of SiPMs changes, 3 M ESR reflective material is added between the contact surface of the scintillator and SiPMs. The reflectivity of ESR can exceed 98%. Taking the opening of 4 SiPMs as an example, the opening in the middle of the array in Fig. 10 is 4 SiPMs receiving windows, and the rest of the reflective parts are increased ESR materials.

9	9	9	8	8	9	9	9
9	8	7	7	7	7	8	9
9	7	6	5	5	6	7	9
8	7	6	1	4	6	7	8
8	7	6	3	2	6	7	8
9	7	6	5	5	6	7	9
9	8	7	7	7	7	8	9
9	9	9	8	8	9	9	9

Fig. 8. Corresponding graphs for different numbers of SiPMs tested (The change of color or increase in number means increased quantity. For example, when 16 slices are selected, all SiPMs 1, 2, 3, 4, 5, and 6 in the figure are included.). (For interpretation of the references to color in this figure legend, the reader is referred to the Web version of this article.)

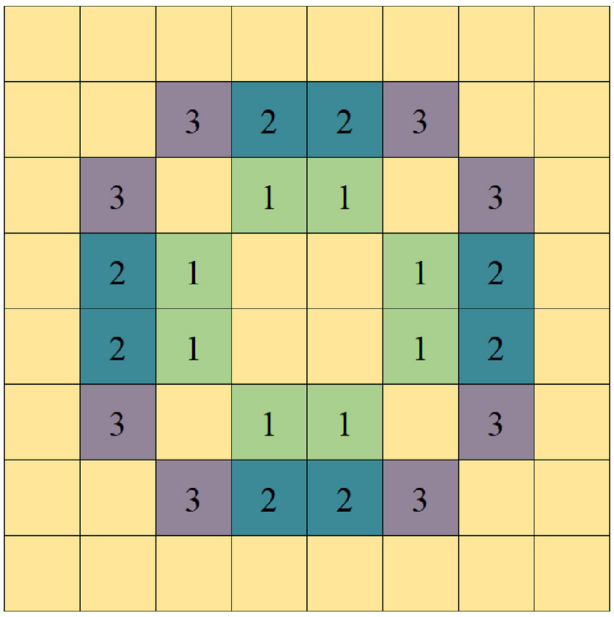

Fig. 9. Corresponding diagram of SiPMs tested at different positions (1, 2, and 3 represent three different positions from the center point).

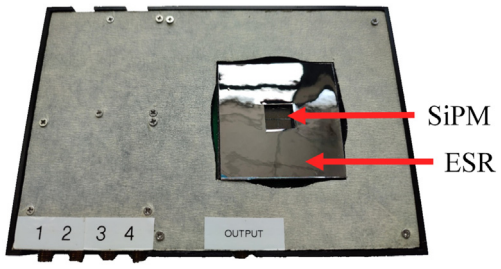

Fig. 10. Add ESR material (reflective part is ESR).

4. Results and discussion

4.1. Quantitative analysis

Fig. 11 shows the energy spectrum measurement of uranium ore after turning on 3 SiPMs. In the figure, the abscissa is the channel, and the ordinate is the logarithmic value of the count. The measurement shown in the figure is compared with the energy spectrum measurement of uranium ore obtained by turning on 64 SiPMs simultaneously (Fig. 7). When only 3 SiPMs are turned on, the main peaks of the uranium ore cannot be distinguished, and the energy calibration cannot be achieved. Therefore, we do not perform an energy spectrum analysis with less than 4 SiPMs.

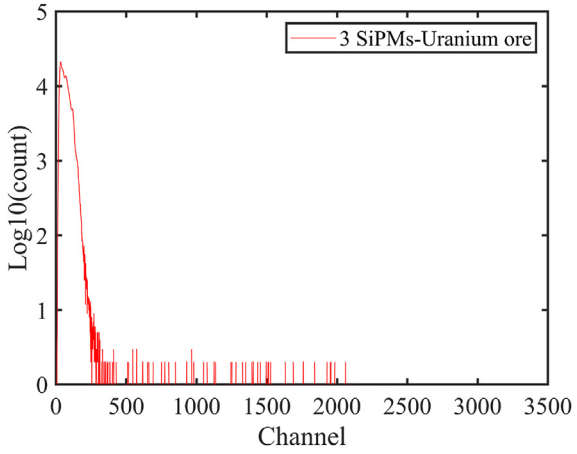

Fig. 11. Uranium ore spectrum with three SiPMs turned on.

Without the reflective film, we find that when the number of SiPMs is reduced by half, the channel corresponding to 662 keV, which in turn corresponds to ^{137}Cs, is also reduced by half. The voltage signal and acquisition generated by SiPMs represent a linear process, such as that shown in Fig. 12. For example, when 32 SiPMs are turned on, the number of channels corresponding to ^{137}Cs after fitting is 520. When the number of SiPMs decreases by half (16 SiPMs), the number of channels corresponding to ^{137}Cs after fitting is 257. At this time, the number of channels is about half of the 32 slices. When the number of SiPMs decreases again, the position of the peak obtained also changes accordingly. The number of channels is obviously not cut in half during the halving process from 64 to 32 because the circular NaI scintillator does not completely cover the square SiPM array. Herein, we set the ordinate to CPS. When the number of SiPMs decreases, the height corresponding to the ordinate increases. Specifically, when reducing the number of SiPMs, the bias voltage does not change; thus, the data accumulate in the direction of the Y-axis, and the Compton plateau of the energy spectrum is superimposed on the characteristic peaks to increase the peak height.

To compare the energy resolutions of the peaks corresponding to 662 keV of ^{137}Cs under different amounts of SiPMs, we need to calibrate the collected data. We select the peaks of the uranium ore corresponding to 609.32, 1120.29, 1764.49, and 2204.06 keV for energy calibration [12] and perform least squares curve fitting on the measured energy calibration data to obtain the following linear equation:

$$\mathrm{E}(x_p) = Gx_p + E_0 \tag{1}$$

where x_p is the peak position, E_0 is the intercept of the straight line, and G is the slope of the straight line that is also known as the gain in the keV/channel [13].

The most important indicator of the quality of the γ spectrometer is the resolution η of the all-power peak of γ. The formula for obtaining η is shown in Eq. (2), where ΔE is the half-width of the all-power peak after energy calibration, and E is the corresponding energy of the highest peak.

$$\eta = \frac{\Delta \mathrm{E}}{\mathrm{E}} \tag{2}$$

Fig. 13 shows the energy spectra of different numbers of SiPMs after calibration with ^{137}Cs. As the number of SiPMs increases, the measured energy resolution also increases, but the relationship between the two is not linear. In the process of increasing the number of SiPMs from 4 to 32, the energy resolution increases from 28.6283% to 10.1461%, and the energy resolution increases by 18%. However, as the number of subsequent SiPMs increases, the improvement of the energy resolution is not particularly obvious. During the change from 32 slices to 64 slices, the energy resolution slightly increases from 10.1461% to 9.8426%. Compared with the 8% gamma spectrometer made by T. Huang et al. [14], our energy resolution is slightly worse because of the absence of coupling between the SiPM array and the scintillator.

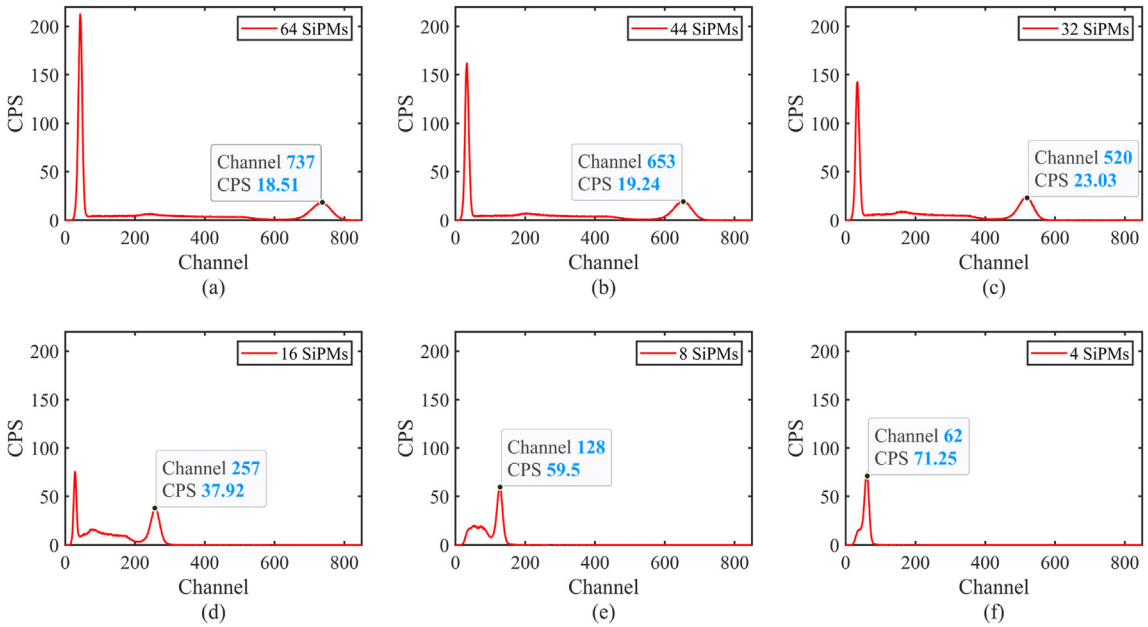

Fig. 12. Energy spectra of 4, 8, 16, 32, 44, and 64 SiPMs without energy calibration (no ESR).

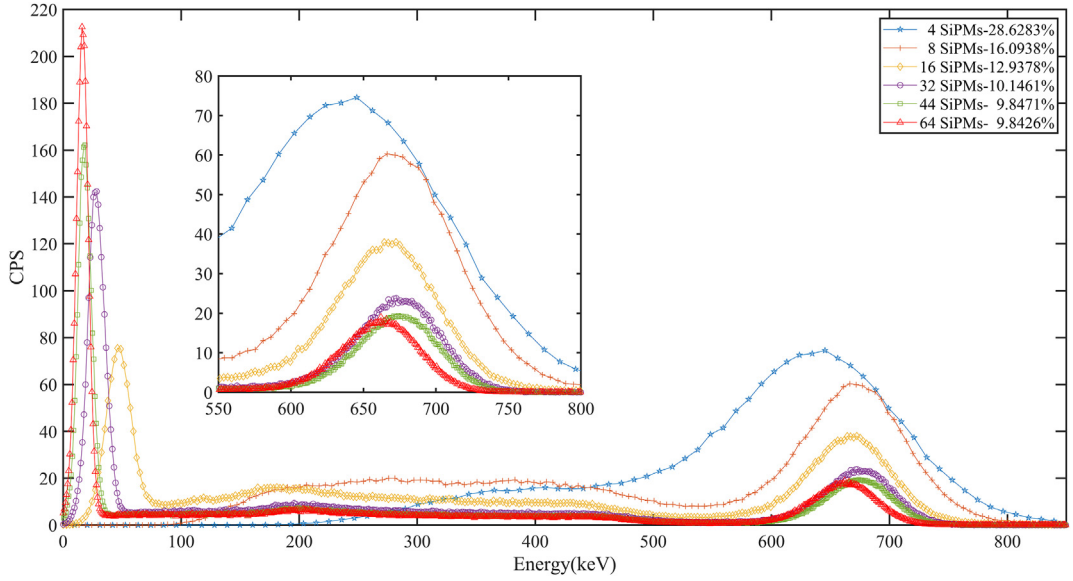

Fig. 13. ^{137}Cs energy spectra after energy calibration for 4, 8, 16, 32, 44, and 64 SiPMs (without ESR; the legend shows the corresponding energy resolution of 662 keV).

4.2. Location result analysis

Fig. 14 shows the energy spectrum obtained by studying the position of SiPMs. By studying the energy resolution of the 662 keV peak of ^{137}Cs, we can conclude that the relative position of SiPMs and the scintillator does not affect the energy resolution of SiPMs. The location experiment also verifies that the reason for the channel halving in Fig. 12 is not caused by location. In the case of different positions, the energy resolution does not change significantly, and the maximum value of ^{137}Cs peak height of 662 keV corresponding to an area farther from the center point becomes slightly large. This result is contrary to those obtained for different numbers of SiPMs. Therefore, the change in peak height corresponding to different numbers is not caused by the relative position of the SiPMs and the scintillator.

4.3. Analysis of the addition of a reflective layer

While adding the reflective layer, we count the effective pulses of 4–64 SiPMs at 120S at ^{137}Cs. The red dot in Fig. 15 is the count after increasing the ESR. Obviously, the number of pulses increases as the number of SiPMs increases. After turning on 32 SiPMs, the total pulse count shows a small increase. When the number of SiPMs remains the same, the addition of the ESR reflective film

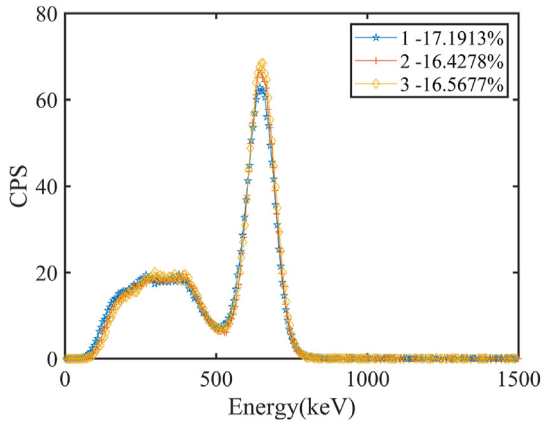

Fig. 14. ^{137}Cs energy spectra of eight SiPMs at different positions (without ESR; the legend shows the corresponding energy resolution of 662 keV).

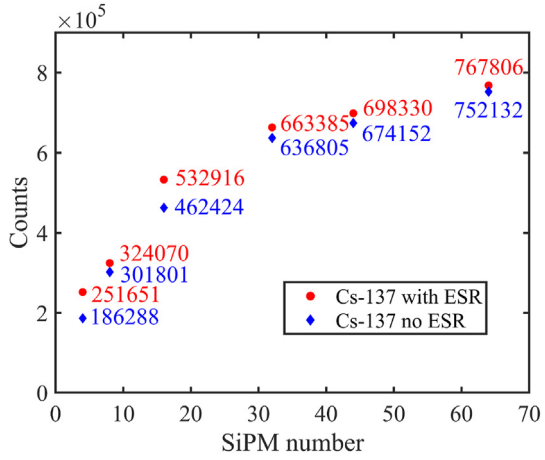

Fig. 15. 120S effective pulse count for different quantities of SiPMs under ^{137}Cs source.

increases the number of effective pulses; that is, the photon collection efficiency increases. For example, at 16 slices, the effective pulse increases by 15.2%. The reason for the increase in the pulse count is that the ESR causes the reflection of scattered photons so that the photons that have not previously acted on the effective SiPMs are collected, thereby increasing the photon count rate.

After increasing the ESR, we continue to measure the ^{137}Cs energy spectra corresponding to different quantities of SiPMs. The energy resolution in Fig. 16 is further improved, but the overall trend of change is consistent with the case in which the ESR is not increased. When the number of SiPMs is small, increasing the ESR improves the energy resolution obviously. This result is explained as follows: when the number of SiPMs that are turned on is small, the area relative to NaI is also small such that a large portion of the photons is not collected by SiPMs. This proportion is large relative to the number of SiPMs. For example, when 4 SiPMs are used, the energy resolution improves by 8.8%; when 16 SiPMs are used, the energy resolution only improves by 0.97%. In the number of groups measured, the energy resolution improves by 10.38% on average. As the increase in the number of SiPMs after the 32nd one has a small improvement in energy resolution, 32 SiPMs can be used to make a gamma spectrometer on the basis of the test results. At this time, the area covered by SiPMs relative to the scintillator is 25.9%. When the energy resolution requirement of the gamma spectrometer is small, 16 SiPMs with increased ESR can be selected. When the number of SiPMs is small, the low-energy peaks in the energy spectrum can no longer be resolved and are not suitable for energy spectrum analysis.

5. Conclusion

We study the relationship between the number and location of SiPMs and the energy resolution of the reflective layer combined with a ⌀ 3 × 3 inch NaI scintillator. The conduction of SiPMs is controlled by each individual mechanical switch, and the effective area of each SiPM is 8 × 8 mm^2. When only the reflective film is added and not coupled, the energy resolution of 662 keV of ^{137}Cs measured by SiPMs reaches 9.8432%. The resolution is poorer than

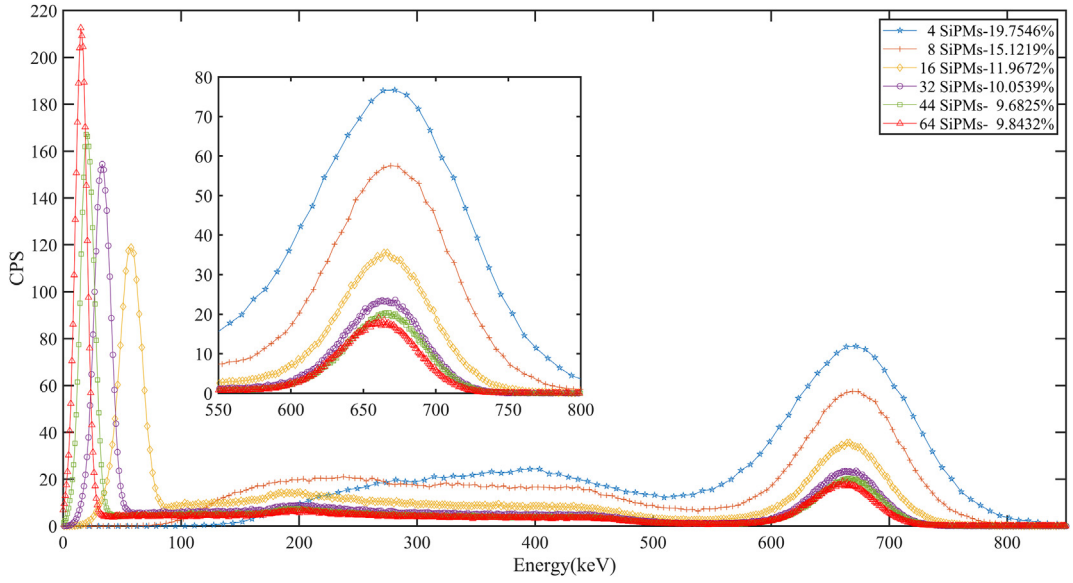

Fig. 16. ^{137}Cs energy spectra after energy calibration for 4, 8, 16, 32, 44, and 64 SiPMs (with ESR; the legend shows the corresponding energy resolution of 662 keV).

most of the current 8% resolution because the coupling between the SiPM array and the scintillator is not performed. When SiPMs are changed from 4 slices to 32 slices, the energy resolution shows a significant improvement. However, the improvement of energy resolution and total pulse count is not obvious, starting from 32 slices (about 25.9% of the area covered by the scintillator). When the number of SiPMs is small, the corresponding energy spectrum cannot be formed. At the same time, we prove that when the SiPM array is completely covered by the scintillator, the position of the SiPMs exerts no significant effect on the energy resolution. However, the addition of the reflective film improves the energy resolution of ^{137}Cs (662 keV) tested by the SiPMs by 10.38% in the measured group on average. Our test results also indicate that directly summing the SiPMs signals results in a decrease in the number of SiPMs and an increase in the CPS value corresponding to the characteristic peak. The influence caused by the position is excluded. The increase of the characteristic peak is caused by the Compton plateau in the front part of the energy spectrum superimposed on the characteristic peak. Our results can provide a reference for the subsequent exploration and development of miniaturized SiPM gamma spectrometers.

Declaration of competing interest

The authors declare that they have no known competing financial interests or personal relationships that could have appeared to influence the work reported in this paper.

Acknowledgments

This work was supported by Defense Industrial Technology Development Program of China (No. JCKY2018401C001), Natural Science Foundation of Jiangxi Province, China (No. 20192BAB202009), Joint Innovation Fund of China National Uranium Co., Ltd. and State Key Laboratory of Nuclear Resources and Environment (No. NRE2021-03), Engineering Research Center of Nuclear Technology Application Mininstry of Education (No. HJSJYB2018-1).

References

[1] I. Mouhti, A. Elanique, M.Y. Messous, Monte Carlo modelling of a NaI (Tl) scintillator detectors using MCNP simulation code, J. Mater. Environ. Sci. 8 (2017) 4560–4565.
[2] J.H. Kim, H.K. Back, K.S. Joo, Development of a wireless radiation detection backpack using array silicon-photomultiplier (SiPM), Nucl. Eng. Technol. 52 (2020) 456–460.
[3] D. Renker, Geiger-mode avalanche photodiodes, history, properties and problems, Nucl. Instrum. Methods Phys. Res., Sect. A 567 (2006) 48–56.
[4] J-series high PDE and timing resolution, TSV package DATASHEET, SensL, Available from: https://sensl.com/downloads/ds/DS-MicroJseries.pdf, 2017.
[5] M. Grodzicka, M. Moszyński, T. Szczęśniak, M. Kapusta, M. Szawłowski, D. Wolski, Energy resolution of small scintillation detectors with SiPM light readout, J. Instrum. 8 (2013) P02017.
[6] C. Kim, H. Kim, J. Kim, C. Lee, H. Yoo, D.U. Kang, M. Cho, M.S. Kim, D. Lee, Y. Kim, Replacement of a photomultiplier tube in a 2-inch thallium-doped sodium iodide gamma spectrometer with silicon photomultipliers and a light guide, Nucl. Eng. Technol. 47 (2015) 479–487.
[7] T. Huang, Z. Zhang, Characterization of 1-inch CLYC scintillator coupled with 8× 8 SiPM array, Nucl. Instrum. Methods Phys. Res., Sect. A 999 (2021) 165225.
[8] Z. Lin, B. Hautefeuille, S.-H. Jung, J. Moon, J.-G. Park, The design of a scintillation system based on SiPMs integrated with gain correction functionality, Nucl. Eng. Technol. 52 (2020) 164–169.
[9] A. Del Guerra, N. Belcari, M.G. Bisogni, F. Corsi, M. Foresta, P. Guerra, S. Marcatili, A. Santos, G. Sportelli, Silicon photomultipliers (SiPM) as novel photodetectors for PET, Nucl. Instrum. Methods Phys. Res., Sect. A 648 (2011) S232–S235.
[10] T. Szcze, M. Grodzicka, M. Moszyński, M. Szawłowski, D. Wolski, J. Baszak, Characteristics of scintillation detectors based on inorganic scintillators and SiPM light readout, Nucl. Instrum. Methods Phys. Res., Sect. A 702 (2013) 91–93.
[11] N. Dinar, D. Celeste, M. Silari, V. Varoli, A. Fazzi, Pulse shape discrimination of CLYC scintillator coupled with a large SiPM array, Nucl. Instrum. Methods Phys. Res., Sect. A 935 (2019) 35–39.
[12] Y. Shigekawa, Y. Kasamatsu, Y. Yasuda, M. Kaneko, M. Watanabe, A. Shinohara, Variation of half-life and internal-conversion electron energy spectrum between U 235 m oxide and fluoride, Phys. Rev. C 98 (2018) 14306.
[13] B. Tang, L. Ge, F. Fang, Y. Liu, Principle of Nuclear Radiation Measurement, Harbin Engineering University Press, 2011.
[14] T. Huang, Q. Fu, S. Lin, B. Wang, NaI (Tl) scintillator read out with SiPM array for gamma spectrometer, Nucl. Instrum. Methods Phys. Res., Sect. A 851 (2017) 118–124.